

# Probability flux as a method for detecting scaling

M. Ignaccolo

*Physics Department, Duke University, Durham (NC)*

P. Grigolini

*Center for Nonlinear Science, University of North Texas, Denton (TX)*

B. J. West

*Information Science Directorate, Army Research Office, Durham (NC)*

(Dated: October 14, 2021)

We introduce a new method for detecting scaling in time series. The method uses the properties of the probability flux for stochastic self-affine processes and is called the *probability flux analysis* (PFA). The advantages of this method are: 1) it is independent of the finiteness of the moments of the self-affine process; 2) it does not require a binning procedure for numerical evaluation of the the probability density function. These properties make the method particularly efficient for heavy tailed distributions in which the variance is not finite, for example, in Lévy  $\alpha$ -stable processes. This utility is established using a comparison with the *diffusion entropy* (DE) method.

PACS numbers: 05.40.-a, 05.45.Tp, 05.40.Fb

## I. INTRODUCTION

Over the past ten years there has been an explosion of research papers published in the area of complex networks. Some would argue that this torrent of publications is a continuance of the growing awareness of complexity science whose origin can be traced back to the decade of the 1960s. The present emphasis on scale-free networks and their implications for scientific disciplines from sociology to neurophysiology had its beginnings with the fractal time series analysis of Mandelbrot [1] and the scaling parameter method of Hurst [2]. From this early appreciation for the limitations of 'normal' statistics to explain and/or characterize complex phenomena we have such terms as 'self-similar', 'self-affine', 'scale invariant',

'fractal', and 'multi-fractal' to capture the non-homogeneous and non-isotropic behavior of statistical variability [3, 4]. As the mathematical developments became more familiar to a generation of scientists the investigations into the manifestations of these effects in biology, economics, geophysics, hydrology, neurophysiology, sociology and so on steadily increased in number. First there were a few isolated studies, followed by a steady rate of overlapping investigations, resulting in what is now a tsunami of monographs, technical papers and popular articles. Consequently, even though no universally accepted definition of complexity has emerged, the consensus of scientific opinion has converged on the use of scaling as one signature of complexity.

The scientific investigations into scaling have historically been of two kinds: 1) the formal mathematics identifying the properties data sequences must possess in order to scale in well-defined ways along with the techniques to analyze the data and reveal that scaling and 2) the application of those techniques to time series measured in complex phenomena. A stochastic process  $X(t)$  is said to scale if the time-dependence of the random variable is such that  $X(t)=K^{-\delta}X(Kt)$  with  $K > 0$  and  $\delta$  is a scaling parameter. Statistical methods to detect self-affinity (scaling) in time series identify the variable  $X(t)$  with the integrated time series and not with the time series itself  $\xi(t)$ , such that,

$$X(t) = \int_0^t \xi(t') dt'. \quad (1)$$

Thus, the original time series  $\xi(t')$  may be viewed as a sequence of increments of the variable  $X$ . In this sense many of the data analysis methods are "diffusive" in that the variable  $X$  is the aggregation of fluctuations denoted by the integral (1). Since its introduction in the middle 1990s *detrended fluctuation analysis* (DFA) [5] has become the method of choice for detecting scaling particularly in biomedical time series [6]. The motivation for introducing DFA was the presumed applicability of the method to non-stationary time series, particularly those with long-time correlations. The scaling methods discussed by Mandelbrot [1] and DFA are "variance" methods in that they assume the time dependence of the variance of the stochastic variable  $Var(X(t))$  with scaling parameter  $\delta$  is algebraic, namely:

$$Var(X(t)) \propto t^{2\delta}. \quad (2)$$

However there are scaling processes such as Lévy flights [7] for which such relationships

are violated because the second moment diverges or Lévy walks [7] for which the second moment is finite and does satisfy a scaling relation similar to (2). The necessity for detecting the proper scaling of Lévy processes was one reason behind the development of the *diffusion entropy analysis* (DEA) method [8] described in Section II. The evident advantage of the information or diffusion entropy  $S(t)$  over second moment methods is that the former is always finite, independently of the behavior of the moments of the probability density distribution (*pdf*)  $p(x, t)$ . The quantity  $p(x, t)dx$  is the probability of finding the trajectory  $X(t)$  in a infinitesimal neighborhood of  $x$  at time  $t$ . The divergence of the central moments, typical of Lévy processes, create difficulties in the numerical determination of the *pdf* and the associated entropy.

Herein we propose a new procedure for determining scaling, the *probability flux analysis* (PFA) as a general method for scaling detection. Since the PFA uses the cumulative probability instead of the density  $p(x, t)$  itself as such it is statistically more efficient than DEA. The cumulative distribution integrates the *pdf* and reduces the noise due to the adoption of a statistical ensemble with a finite number of trajectories. The PFA method is shown to outperform the other methods in the case of Lévy processes. The present paper is structured as follows. In Section II we introduce scaling for the *pdf*, which is an extension of the concept of self-affinity. Ordinarily self-affinity is recovered in the algebraic time dependence of a scaling function  $\beta(t)$  as we show using the DEA method and its numerical implementation. We introduce the PFA method in Section III, and compare its performance with that of DEA on computer generated time series in Section IV and subsequently make the same comparisons with real world data. Finally, we draw some conclusions in Section V.

## II. SCALING

Consider a one-dimensional stochastic trajectory  $X(t)$  whose statistical properties are described by  $p(x, t)$ . The stochastic process represented by  $X(t)$  is said to scale if the corresponding *pdf* satisfies the scaling relation

$$p(x, t) = \frac{1}{\beta(t)} F\left(\frac{x}{\beta(t)}\right) \quad (3)$$

where the scaling function  $\beta(t)$  is a function of time and without loss of generality we have assumed  $X(0) = 0$ . The function  $F$  in the above equation is the scaled density since

$$\int p(x, t) dx = \int F(y) dy = 1. \quad (4)$$

The relation (3) proposed here is a generalization of the widespread notion of scaling adopted in the literature [3, 4], which often corresponds to the particular case

$$\beta(t) = t^\delta. \quad (5)$$

Herein we refer to the validity of the scaling relation (3) together with (5) as the ‘‘algebraic’’ scaling condition. Geometrically, the scaling condition implies that  $p(x, t)$  is invariant under the transformations

$$\begin{cases} x \rightarrow \frac{\beta(t)}{\beta(Kt)}x \\ t \rightarrow Kt \end{cases} \Leftrightarrow X(t) \underset{s}{=} \frac{\beta(t)}{\beta(Kt)} X(Kt) \quad (6)$$

where  $K > 0$  and the symbol  $\underset{s}{=}$  denotes equality in the sense that the *pdfs* for the variables on either side of the equal sign are the same. In the case of algebraic scaling ( $\beta(t) = t^\delta$ ) we have

$$\begin{cases} x \rightarrow K^{-\delta}x \\ t \rightarrow Kt \end{cases} \Leftrightarrow X(t) \underset{s}{=} K^{-\delta} X(Kt). \quad (7)$$

This last set of relationships defines a self-affine transformation [3].

### A. Scaling detection with Diffusion Entropy Analysis (DEA)

The *pdf* defined for the stochastic process  $X(t)$  can be used to calculate the information entropy. This use of entropy was implemented in discrete form for coding information by Shannon [9] and is referred to as the Shannon entropy. Contemporaneously, this use of entropy was introduced in continuous form by Wiener for studying the problem of filtering noise from messages in electrical circuits [10]. In the analysis here we use the continuous form of information entropy

$$S(t) = - \int p(x, t) \log_2 p(x, t) dx, \quad (8)$$

which was originally identified as diffusion entropy by Scafetta *et al.* [8] as a tool for detecting scaling in time series. The advantages of using entropy rather than the variance to detect

scaling is that entropy provides a more complete description of the stochastic process. The two approaches become equivalent only when the *pdf* is Gaussian. In the general case the distribution is not Gaussian and the central moments can and do diverge, as in the case of  $\alpha$ -stable Lévy distributions. If the scaling condition (3) is satisfied then it is straightforward to show that the entropy reduces to

$$S(t) = S_0 + \log_2 \beta(t), \quad (9)$$

while in the case of algebraic scaling, given by Eq. (5), we have

$$S(t) = S_0 + \delta \log_2 t, \quad (10)$$

where the additive constant is defined by the integral over the scaled variable

$$S_0 = - \int F(y) \log_2 F(y) dy. \quad (11)$$

The empirical determination of the histograms replacing the *pdf*'s and the discretization of the integral (8) is done as follows. A discrete realization  $X_l$  ( $l=0,1,2,\dots,N$ , and  $X_0=0$ ) of the stochastic process  $X(t)$  is used to create the set of trajectories

$$\{X_k(t)\} = \{X_{k+t} - X_k\} \quad k = 0, 1, 2, \dots, N - t. \quad (12)$$

We call the set  $\{X_k(t)\}$  of  $N - t + 1$  trajectories the Single Trajectory Ensemble (STE) as distinct from the Multiple Trajectory Ensemble (MTE) generated using  $N - t + 1$  different realization of the stochastic process  $X(t)$ . The rationale for the STE is that in many real world applications one has only a single realization of the stochastic process available. The two ensembles are generally thought to produce identical results when the stochastic process is stationary and ergodic; even in the non-stationary case the STE and MTE averages are thought to be the same provided the effect of local trends can be eliminated, *e.g.*, by using the DFA algorithm [5]. However, the equivalence between STE and MTE is lost even in the stationary and ergodic case [11], and caution must be used when interpreting the results of scaling analysis that rely on the STE. The procedure described in Eq. (12) to generate the STE has been called the ‘‘overlapping’’ windows method as two trajectory  $X_{k_1}(t)$  and  $X_{k_2}(t)$  may share a common profile if  $|k_2 - k_1| < t$ . The overlapping windows method is often preferred to the non-overlapping windows methods because of the larger number of trajectories produced [12].

In the present manuscript the STE is used to calculate the histogram for the *pdf*  $p_{j,\Delta}(t)$  for finding a trajectory within an interval of size  $\Delta$  centered on the value  $x_j$ . The bin size  $\Delta$  has to be sufficiently small to consider the *pdf* constant within the interval  $[x_j - \Delta/2, x_j + \Delta/2]$ , and the integral of Eq. (8) can then be approximated by the sum

$$S(t) \simeq - \sum_{j=1} p_{j,\Delta}(t) \log_2[p_{j,\Delta}(t)] + \log_2 \Delta. \quad (13)$$

The accuracy of this numerical approximation decreases as  $t$  increases since we have only  $N-t+1$  of trajectories in the STE. Values of the density  $p(x, t) \sim 1/(N-t+1)$  are impossible to reproduce correctly. Moreover, if the stochastic process  $X(t)$  is such that the probability of observing large values, positive and/or negative, increases in time than the *pdf* will assumes increasingly smaller values further compromising the validity of Eq. (13). This effect is particularly dramatic when the stochastic process has infinite second and and/or first moment such as the Lévy flights and walks considered in Section IV.

### III. SCALING DETECTION WITH PROBABILITY FLUX ANALYSIS (PFA)

The rationale for the *probability flux analysis* (PFA) is to have a method of scaling detection that is independent of the binning procedure used to evaluate the histogram for the *pdf*, statistically more accurate, and independent of the size of the moments of the distribution. Define a constant in the interval  $\theta \in ]0, 1[$  and  $x_\theta(t)$  to be a number such that

$$\theta = \int_{-\infty}^{x_\theta(t)} p(x', t) dx' \equiv \mathcal{P}(x_\theta(t), t) \quad \forall t, \quad (14)$$

where  $\mathcal{P}(x, t)$  is the cumulative distribution. The value of the variate  $x_\theta(t)$  encompasses a fraction  $\theta$  of the probability density  $p(x, t)$ . We call PFA any algorithm that at any time step  $t$  calculates the number  $x_\theta(t)$ .

If the scaling condition on the *pdf* (3) is satisfied,

$$\mathcal{P}(x, t) = \int_{-\infty}^x p(x', t) dx' = \int_{-\infty}^x \frac{1}{\beta(t)} F\left(\frac{x'}{\beta(t)}\right) dx' = \mathcal{F}\left(\frac{x}{\beta(t)}\right) \quad (15)$$

where the function  $\mathcal{F}$  is the cumulative distribution of the scaled density  $F$ . Thus, for a scaling *pdf* the condition (14) becomes

$$\theta = \mathcal{F}\left(\frac{x_\theta(t)}{\beta(t)}\right) \quad \forall t \Rightarrow x_\theta(t) = z_\theta \beta(t) \quad (16)$$

where  $z_\theta$  is a constant. This equation shows that in the case of scaling the motion in time of the location  $x_\theta$  with a fraction  $\theta$  of the trajectories  $X(t)$  on its left side is directly proportional to the motion described by the scaling function  $\beta(t)$ . In case of algebraic scaling, Eq. (3) and Eq. (5),

$$x_\theta(t) = z_\theta t^\delta \Rightarrow \ln[x_\theta(t)] = \ln(z_\theta) + \delta \ln(t) \quad (17)$$

In the case of a constant drift, Eqs. (14)–(17) are valid in the moving reference frame centered on  $\omega t$ , or equivalently for the variable  $x_\theta(t) - \omega t$  instead of  $x_\theta(t)$ . As an example, let us consider the stochastic process  $X(t)$  to be Brownian motion with no drift, then the *pdf*  $p(x, t)$  is a Gaussian function centered on the origin  $x=0$ , while the scaling function  $\beta(t)=\sqrt{t}$ . Consider  $\theta=0.977$  that is  $x_{0.977}$  encompasses 97.7% of the distribution. For a Gaussian distribution  $x_{0.997}$  correspond to a value in excess of two standard deviation from the mean. Thus for a Brownian motion with no drift  $x_{0.997}(t)=2\sigma\sqrt{t}$  which satisfies the second relation of Eq. (16) with  $z_\theta=2\sigma$ ,  $\sigma$  being the standard deviation of the increments of  $X(t)$ .

The numerical calculation of the function  $x_\theta(t)$  can be done as follows. At any time  $t$  the trajectories  $\{X_k(t)\}$  of the STE defined in Eq. (12) are placed in ascending order and the value  $x_\theta(t)$  is assigned to be  $X_K(t)$  with  $K=[\theta \times (N - t + 1)]$ ,  $[..]$  indicating the integer part. This procedure requires no binning as the DEA algorithm, however it can be computationally demanding since at any time step  $t$  the trajectories  $\{X_k(t)\}$  must be sorted. Hereby, we use a faster procedure. We estimate  $x_\theta(t)$  by calculating the cumulative distribution  $\mathcal{P}(x, t)$  at fixed spatial intervals of length  $\Delta$ : the accuracy (resolution) with which the value  $x_\theta(t)$  is computed. Let  $\{X_k(t)\}$  be the set of trajectories of the STE at time  $t$ , and  $M(t)$  the total number of bins of length  $\Delta$  necessary to cover the span of these trajectories, we define  $x_\theta(t)$  as follows

$$x_\theta(t) = x_l \text{ such that } \sum_{j=1}^l p_{j,\Delta}(t) < \theta \text{ and } \sum_{j=l+1}^{M(t)} p_{j,\Delta}(t) > \theta \quad (18)$$

where the symbol  $p_{j,\Delta}(t)$  indicates the trajectory frequency or histogram within the  $j$ -th interval  $[x_j - \Delta/2, x_j + \Delta/2]$ . Calculating the frequencies  $p_{j,\Delta}(t)$  requires a single sequential scanning of the trajectories  $\{X_k(t)\}$  while any sorting algorithm requires more computational power. The procedure described by Eq. (18) is similar to the DEA algorithm (13) as both methods require the calculation of  $p_{j,\Delta}(t)$ . However, there is a fundamental difference. For the DEA to be meaningful  $p_{j,\Delta}(t)/\Delta$  must accurately reproduce the *pdf* in each interval.

This strong requirement is not necessary for the method described in (18). The adoption of a binning procedure in the case of PFA is just a computational device to speed up calculation.

#### IV. COMPARISON BETWEEN PFA AND DE METHOD

In this section, we compare the results of the PFA and DEA methods applied to a number of computer generated sequences having known statistical properties. In addition we apply the two techniques to the electroencephalogram (EEG) data set previously analyzed [14].

##### A. Lévy Flights

In this section we generate a number of Lévy flights for the stochastic process  $X(t)$ . These processes have stationary delta-correlated increments  $\xi(t)$  with infinite variance and possibly also infinite mean depending on the value of the Lévy index selected. The generalized central limits theorem predicts the *pdf* to be, after an initial transient that depends on the specific distribution of the increments, a Lévy distribution. The function  $F(y)$  on the right hand side of Eq. (3) is a stable Lévy distribution whose Fourier transform is given by

$$\mathcal{F}(k) = \exp [ ik\gamma - |ck|^\alpha (1 - i\eta \operatorname{sgn}(k)\Phi) ]. \quad (19)$$

In the above equation  $\mathcal{F}(k)$  is the characteristic function of  $F(y)$ ,  $\gamma \in \mathcal{R}$  is the shift parameter,  $\eta \in [-1,1]$  is called the skewness parameter, a measure of asymmetry, and  $0 < \alpha \leq 2$  is the Lévy parameter. Finally, the constant  $\Phi$  is equal to  $\tan(\pi\alpha/2)$  for all values of  $\alpha$  except for  $\alpha=1$  when  $\Phi=(2/\pi) \log |k|$ .

We choose the increments  $\xi$  of the variable  $X$  to be distributed according to an inverse power law

$$\psi(\xi) = \frac{(\mu - 1)B^{(\mu-1)}}{(B + |\xi|)^\mu} \quad (20)$$

where  $\mu \in ]1, +\infty[$  is the “index” of the inverse power law and  $B \in \mathcal{R}$  is a location parameter ( $\xi \gg B \Leftrightarrow \psi(\xi) \propto |\xi|^{-\mu}$ ). The scaling parameter  $\delta$  of the resulting Lévy distribution for  $p(x, t)$ , the power law index  $\mu$ , and the Lévy parameter  $\alpha$  are connected as follow:

$$\alpha = \mu - 1 \quad \text{and} \quad \delta = \frac{1}{\alpha} = \frac{1}{\mu - 1} \quad \text{for } \mu \in ]1, 3[. \quad (21)$$

where, of course,  $\alpha=2$  corresponds to the Gaussian distribution, which we do not consider here. Random numbers distributed according to (20) can be obtained from random numbers

uniformly distributed in the interval  $]0,1[$  [15]. To test the performance of PFA and DEA on Lévy flights, we generate  $10^7$  random numbers distributed according to the inverse power law Eq. (20) with location parameter  $B = 1$  and power law index  $\mu = 1.6$ . The result are recorded in figures below.

We see from the calculation depicted in Figure 1 that both the DEA and PFA methods apparently provide reliable estimates of the early time scaling of the stochastic process, even though we have only used the first 25% of the data in the use of PFA. The slope of the curves in both calculation is  $1.\bar{6}$ , the expected scaling index  $\delta$  in (21). However after two decades the DEA curve begins to run out of statistics, whereas the PFA persists for another decade and one-half before it markedly deviates from the theoretical curve. The detailed divergence between the two calculations is evident in the insert.

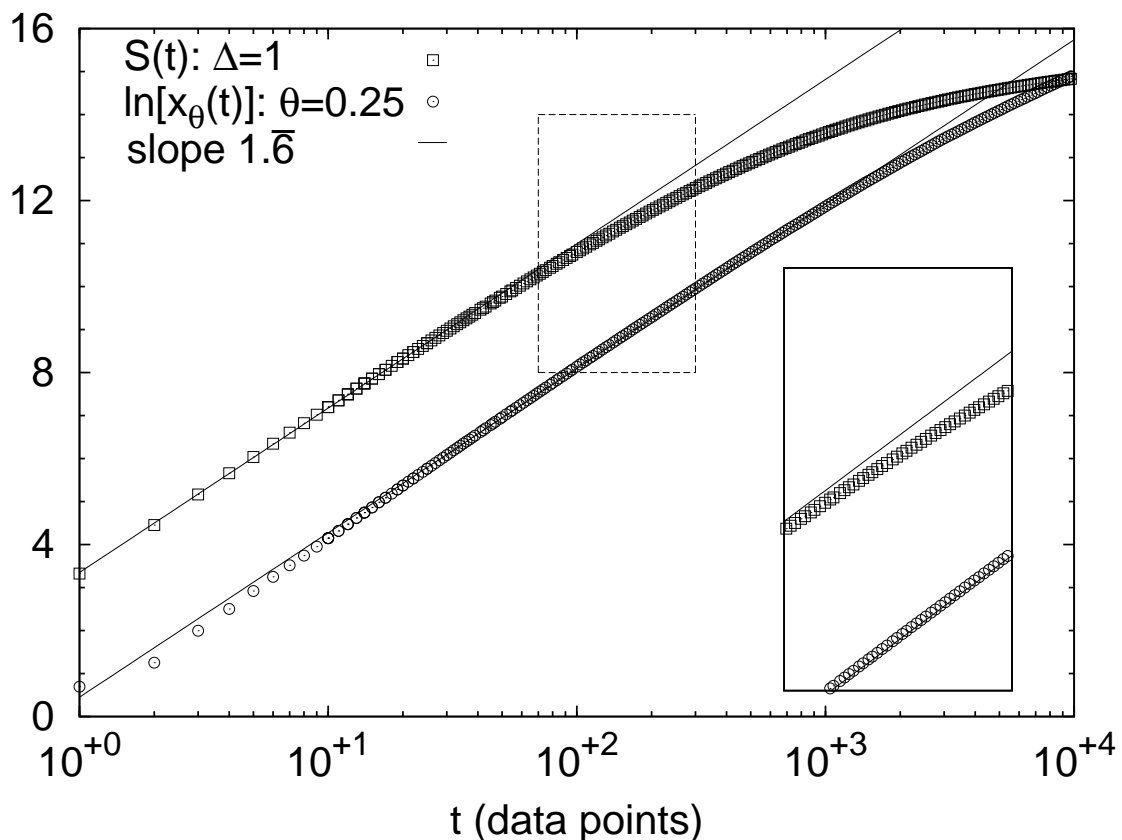


FIG. 1: Figure 1: Probability Flux Analysis (PFA) and the Diffusion Entropy Analysis (DEA) are graphed for  $10^7$  computer-generated data points using (20) with a Lévy flight of scaling index  $\delta = 1.\bar{6}(\mu = 1.6)$ .

In Figure 2a the *pdf* is depicted at times  $t = 50$  and  $t = 10^3$ , with the latter vertically dis-

placed for visual clarity. In the vicinity of the first time both the DEA and PFA calculations have the same slope as that of theory, whereas in the vicinity of the latter time the DEA calculation significantly deviates from the theoretical curve and the PFA calculation does not. The *pdf* at  $t = 50$  loses its crispness for large values of the variate where the process becomes undersampled and therefore fluctuates significantly from value to value. On the other hand, the *pdf* at  $t = 10^3$  is undersampled throughout the domain of the distribution and therefore the weight of successive values of the histogram are quite noisy. This is what is meant by "running out of statistics" in the DEA calculation in Figure 1; there is insufficient statistics to reduce the noise in the histogram. The DEA calculation therefore is more useful at early times where the histogram for the *pdf* is more reliable. At latter times the larger values of the variate become increasingly more important and the histograms becomes increasingly less reliable. However, this lack of reliability in the histograms has no apparent influence on the PFA since slope determination with this latter method is done only using those values of the variate below the percentage cut off  $\theta$  and not on a faithful reproduction of the *pdf* in the entire range of the variate.

Another way of comparing the distribution at different times is to examine the survival probabilities. Lévy distributions (with the exception of the Gaussian case  $\alpha = 2$ ) have inverse power-law tails with index  $\alpha + 1$ . Thus, the corresponding survival probability has an inverse power-law tail with index  $\alpha$ . In Figure 2b, we see that at  $t = 50$  the slope of the inverse power-law survival probability ( $\alpha = \mu - 1 = 0.6$  in our case) coincides with the theoretical curve over multiple decades of variate values. The extended inverse power-law region of the survival probability is indicative of the quality of the *pdf* depicted in Figure 2a. On the other hand, the  $t = 10^3$  survival probability does not have a region that coincides with the theoretical inverse power law for any values of the variate. This lack of scaling is consistent with what is observed from the DEA calculation in Figure 1. The empirical survival probability is not sufficiently robust to detect the scaling in the data at late times. However the survival probability is statistically robust at the  $1 - \theta$  level and thus the PFA method continues to detect the scaling.

To drive home this point it is useful to examine how the PFA depends on the choice of  $\theta$ . In Figure 3 we plot the residue of the PFA analysis for four widely spaced values of the fraction  $\theta$  using the same computer-generated data of Figure 1 and 2 ( a Lévy flight index  $\alpha=1.\bar{6}$  ;  $\mu=1.6$ ). The calculation tracking the theoretical slope for the longest time

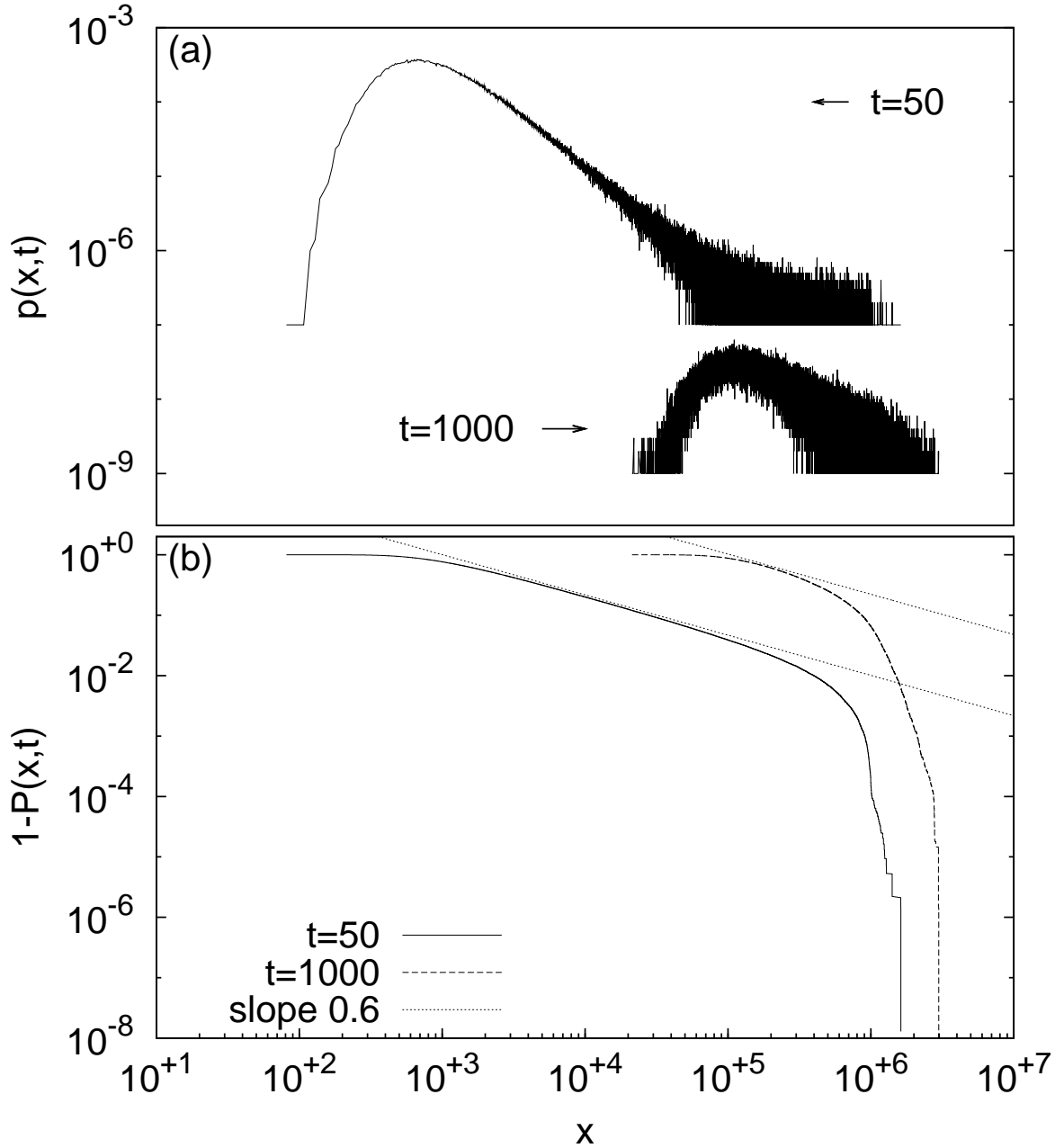


FIG. 2: Figure 2:(a) The *pdf* is given at times  $t = 50$  and  $10^3$ . It is evident that  $p(x, t)$  is better at earlier times indicating that this is where the DEA will be most useful. (b) The survival probability at the two times is depicted. At  $t = 50$  the survival probability is an inverse power law for more than two decades, whereas at  $t = 10^3$  there is essentially no region where a theoretical inverse power law is detected.

$t = 10^4$  has  $\theta = 0.05$ . As the "time"  $t$  increases the number of trajectories  $N - t + 1$  available in the STE decreases. Therefore the larger  $\theta$  the earlier in time the cumulative (survival) probability  $(1 - \theta)$  becomes statistically unreliable. The divergence of the first and second moments in the Lévy flight considered here makes this loss of statistical robustness even more dramatic. A similar effect will also occur if very small values of  $\theta$ , for example,  $\theta \ll 0.01$ , are adopted. In fact, although the support of the *pdf* is  $[0, \infty]$ , the left border of the support of its numerical approximation can be several orders of magnitude larger as shown in Figure 2

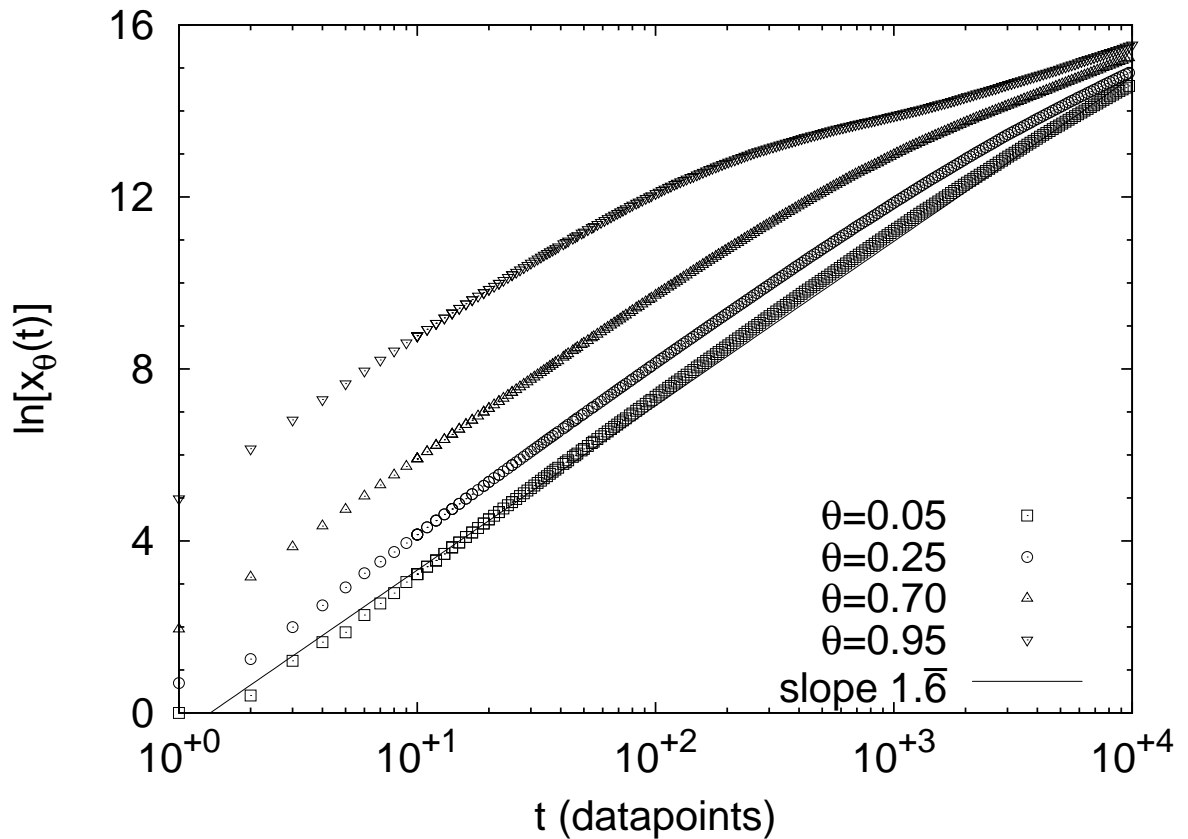


FIG. 3: Figure 3: The PFA calculation is graphed for  $10^7$  computer-generated data points using (20) with a Lévy flight of index  $\alpha = 1.\bar{6}$  ( $\mu = 1.6$ ) for a number of different values of  $\theta$ .

### B. Lévy walks

A random walk is a stochastic process  $X(t)$  where the distance covered by the walker, the value of the variate, in a finite time is limited. The restriction on the walk is a consequence

of the physical relation between taking a step of a given size and the time required to take such a step [7]. Hence, at any given time  $t$  the walk *pdf* is bounded and all the moments are finite. A Lévy walk has a *pdf* between the fastest walkers that is approximately equal, after a transient, to a Lévy distribution. Lévy walks can be generated in a number of different ways, for example, using chaotic intermittent maps [16], or, as we will do herein, using inverse power-law distributed random numbers. We consider a type of Lévy walk called the Symmetric Velocity Model (SVM) [16]. In the SVM walk, the velocity of the random walker can only assume two values/states, here taken to be  $\pm 1$ . The velocity of the walker remains in a given state for an interval of time of random duration  $\tau$  distributed according to the waiting-time distribution density  $\psi(\tau)$  given by the inverse power-law distribution (20) with index  $\mu \in [2, 3]$ . After waiting in a given state for a time  $\tau$ , that is, traveling at a constant velocity for the specified time interval, a coin is tossed to determine the new value of the velocity; and a new  $\tau$  is extracted from the distribution  $\psi(\tau)$  to determine the duration of this new velocity value. The pdf of the SVM walk at time  $t$  is bounded between  $[-t, t]$  and can be approximated ( $t \gg$  mean time of  $\psi(t)$ ) by the scaling expression Eq.(3) with  $F(y)$  being a symmetric Lévy stable distribution with shift parameter given by  $\gamma = 0$ , the skewness parameter  $\eta = 0$ , Lévy index  $\alpha = \mu - 1$ , and by using the scaling function  $\beta(t) = t^{1/\alpha}$  [8, 16].

For the numerical implementation of the SVM walk, we extract  $10^6$  random waiting times  $\tau$  according to the inverse power-law distribution with index  $\mu = 2.5$  and location parameter  $B = 1$ . Then we consider the transformation  $\tau \rightarrow [\tau] + 1$  where  $[.]$  is the integer part of the term in brackets. This transformation creates a sequence of integers  $\{\tau_k > 0\}$ , which are inverse power-law distributed with the same index  $\mu$  and approximately the same location parameter  $B$  of the original sequence. To assign the velocity states we generate a  $10^6$  long sequence of random coin tosses:  $\{v_j = \pm 1\}$ . Finally we use the couples  $\{\tau_j, v_j\}$  to create the sequence  $\xi_j$  of increments (the velocity of the walker) of the stochastic variable  $X$  and consequently the sequence  $X_j$ , which is processed using the DEA algorithm.

In Figure 4 the PFA calculations for the four different values of  $\theta$  are compared with the DEA calculation. After an initial transient ( $t \sim 10^2$ ), the DEA calculation tracks the theoretical straight line ( $S(t) \propto \delta \ln t$  with  $\delta = 1/(\mu - 1) = 0.6$ ) up to a time  $t \lesssim 10^4$  after which the DEA begins to run out of statistics. The *pdf* of the SVM walk is symmetric, however the numerical evaluation may not be symmetric, and at any time step we subtract

the numerical mean before calculating the value of  $x_\theta(t)$ , which satisfies Eq. (14). Moreover due to the symmetry of the SVM walk  $x_{\theta=0.5}(t) = 0$ , and  $x_{\theta_1}(t) = -x_{\theta_2}(t)$  if  $|\theta_1 - 0.5| = |\theta_2 - 0.5|$ , that is, if the two different values of the parameter  $\theta$  are symmetric with respect to 0.5. Therefore, we limit ourselves to doing the PFA calculations for  $\theta > 0.5$ . The results depicted in Figure 4 indicate that PFA tracks the theoretical straight line for an additional decade beyond that of DEA. The results are approximately independent of the particular value of the cut off fraction  $\theta$ , although larger values show less wiggly behavior than do smaller ones; an effect seemingly at odds with those found in the previous case of the Lévy flight. The rationale for this effect is the following. For the SVM Lévy walk,  $x_{\theta=0.5}(t) = 0$  for all  $t$ , however for the numerical calculation this is not true and a plot of  $x_{\theta=0.5}(t)$  reveals a fluctuating value. The fluctuations increase in intensity as the time  $t$  increases since the number of trajectories in the STE decreases as  $N - t + 1$ , and the *pdf* becomes less symmetric. The cut off location  $x_\theta(t)$  for values of  $\theta$  closer to 0.5, such as 0.6 are more affected by this type of noise than the cut off location for larger values of  $\theta$  such as 0.9. The overall effect is that although in theory  $x_{\theta=0.6}(t)$  should be more robust than  $x_{\theta=0.9}(t)$ , in practice, the latter is "crisper" than the former.

### C. EEG records

In the previous two subsections we compared the results of using the DEA and PFA methods to determine the known scaling properties of computer-generated data sets having diverging and finite second moments, respectively. Now we turn our attention to experimental data sets whose unknown scaling properties we wish to determine. One such data set of both historic and contemporary interest is that of the electroencephalogram (EEG) depicting the erratic dynamics of the human brain. The observed scaling in EEG time series is not as straightforward as observed in other less complex phenomena. Various measures other than the standard deviation and spectrum have been introduced into the study of EEG time series, each one stressing a different physiologic property thought to be important in representing the brain's dynamics. Most recently the DEA method has revealed a rather remarkable behavior of the single channel EEG time series. Specifically the failure of the EEG signal to scale: e.g.: Hwa et al.[18] applied DFA to the series of increments of EEG increments and found a bi-scaling regime. Ignaccolo *et al.* [14] argues that the EEG signal

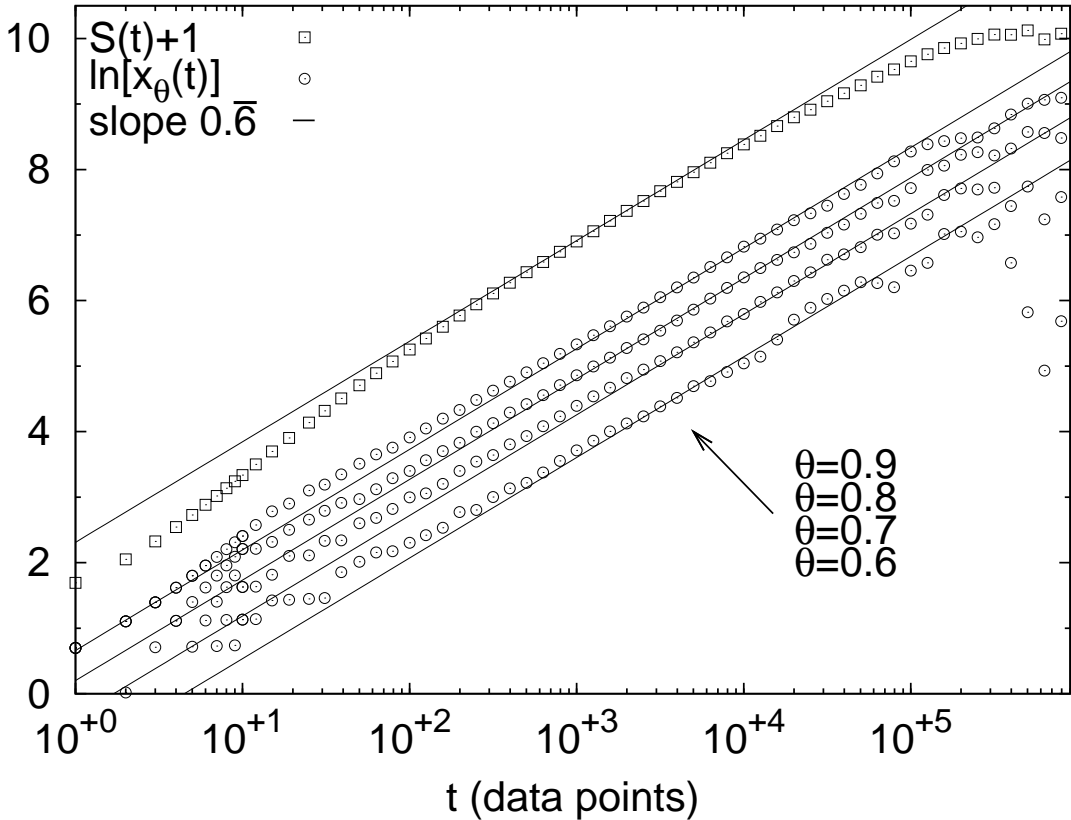


FIG. 4: Figure 4: The DEA and PFA calculations for a Lévy walk for four values of the fraction of the data included in the calculation.

during resting activity can be modeled using a dissipative linear dynamic process  $X(t)$ , i.e., an Ornstein-Uhlenbeck process, with a quasi-periodic driver having a random amplitude and frequency and an additive random force  $\eta(t)$  which is a delta correlated Gaussian process of strength  $\sigma$ . Latka *et al.* [19] shows how the model proposed in [14] explains the bi-scaling regime observed by Hwa *et al* [18] and why this is not a “real” algebraic scaling regime (satisfying Eqs. (3) and (5)) but is an artefact of DFA.

Fig. 5 shows the DEA for an EEG channel under the closed eyes resting condition. The time  $t$  is expressed in seconds with 1 second corresponding to 250 data samples. The observed saturation is the results of dissipative linear dynamics while the decaying oscillations are produced by the random periodic forcing: the alpha rhythm which is the well known wave pattern present in EEG under the closed eyes resting condition. Different trajectories of the STE (12) experience wave packets of different amplitude and frequency. The typical duration of a wave packet is  $\sim 0.5$ s [14]. The mixture of wave packets results in a pattern of

destructive interference. The larger the time  $t$ , the wider the spectrum of different amplitudes and frequencies present in the trajectory  $X_k(t)$  of Eq. (12), and the more intense is the interference. This mechanism explains the observed decaying oscillation for the information entropy  $S(t)$ . The apparent period  $\sim 0.013$ s is just the amplitude weighted average of  $\alpha$ -wave packet periods occurring in the particular EEG record examined. Also plotted in Fig.5 is the PFA for different values of the cut off fraction  $\theta$ . We see how PFA reproduces all the characteristic observed for DEA. Note that EEG records are almost symmetric so that the PFA analysis for  $\theta < 0.5$  is just the mirror image of the one shown, as is the Lévy SVM walk of the previous section, of the one relative to  $\theta > 0.5$ . This also explain why the results are increasingly “crisp” when moving from  $\theta = 0.6$  to  $\theta = 0.9$  in Fig. 5.

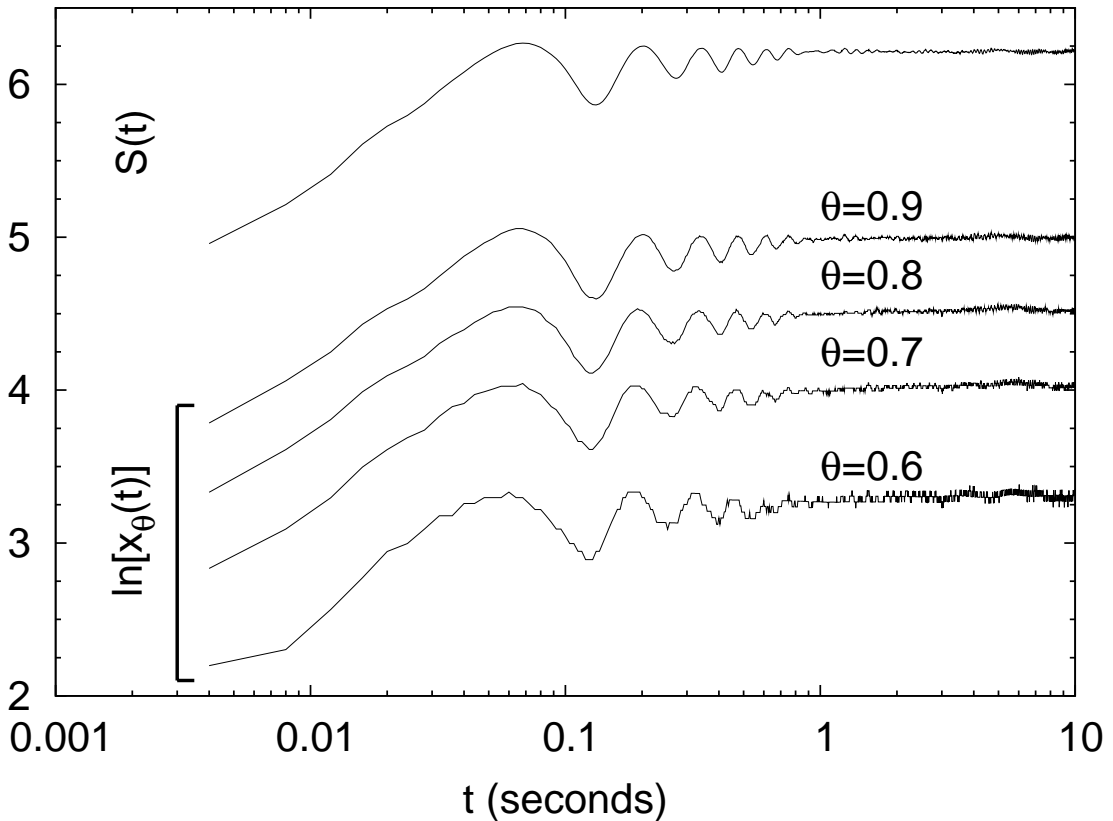


FIG. 5: The DEA processing of the EEG data from a single channel in the occipital lobe is labeled  $S(t)$ . The equivalent PFA processing of the same data using four different values  $\theta$  is also shown.

## V. CONCLUSION

The PFA calculates the “cut off” location  $x_\theta$  which encompasses a fraction  $\theta$  of the *pdf* of the stochastic process  $X(t)$ . As the *pdf* evolves in time so does  $x_\theta$  in order to always encompass the same fraction of the distribution. In this sense, PFA is a “volume” preserving transformation. The volume preserving transformation for a scaling distributions is, aside from a constant multiplicative factor, the scaling function itself (16). Therefore PFA can be a scaling detection tool. The power of this method is that the volume preserving transformation is statistically more robust than any method based on a detailed knowledge of the *pdf* such as DEA. The PFA with cut off fraction  $\theta$  is as statistically robust as the cumulative distribution  $\mathcal{P}(x, t)$  at level  $\theta$  or the survival distribution  $(1 - \mathcal{P}(x, t))$  at level  $(1 - \theta)$ . For a bounded signal with a “well-behaved distribution” (no inverse power law with infinite first or second moment) such as the EEG data the statistical advantage of the PFA over DEA may not be so evident (Fig. 5). However, as soon as we depart from the realm of well-behaved distributions the statistical advantage of PFA becomes apparent. For the SVM Lévy walk the agreement with the theoretical curve is extended by one decade (Fig. 4). SVM Lévy walks have bounded *pdf*'s but a non well-behaved distribution is hidden in this stochastic process: the *pdf* of the waiting times (20) with index  $\mu \in ]2, 3[$ , which has an infinite variance, and is the reason why a Lévy distribution appears in the region between the bounding sites. The statistical advantage of PFA over DEA is even more evident in the case of Lévy flights where the *pdf* is unbounded with infinite first and second moments. In this latter case, almost two decades are gained using one method rather than the other (Fig. 1 and 3).

Aside from scaling detection, the results of Fig. 5 relative to the EEG record, where there is no algebraic scaling, shows that PFA can be used to investigate the dynamics of a stochastic process  $X(t)$ . In fact, the details of the dynamics generating the signal  $X(t)$  are somewhat reflected in the volume preserving transformation performed by PFA. From these results the inescapable conclusion is that the PFA method is superior to the DEA and ought to replace it. Moreover, since we have shown elsewhere [14] that DEA is preferable to detrended fluctuation analysis (DFA), we must further conclude that PFA replace DFA as well.

M. I. and B. J. W. thank the Army Research Office for support of this research.

- 
- [1] B.B. Mandelbrot, *Fractals; form, chance and dimension*, W.H. Freeman and Co., San Francisco (1977).
- [2] H.E. Hurst, *Trans. Am. Soc. Civil Eng.* **116**, 770-808 (1951).
- [3] J. Feder, *Fractals*, Plenum Press, New York (1988).
- [4] M. Schroeder, *Fractals, chaos, power laws*, W.H. Freeman, San Francisco (1991).
- [5] C. K. Peng, S.V. Buldyrev, S. Havlin, M. Simons, H. E. Stanley and A. L. Golberger, *Phys. Rev. E*, **49**, 1685 (1994).
- [6] J.B. Bassingthwaite, L.S. Liebovitch and B.J. West, *Fractal Physiology*, Oxford University Press, Oxford (1994).
- [7] M.F. Shlesinger, J. Klafter and B.J. West, *Phys. Rev. Lett.* **58**, 1100-03 (1987).
- [8] N. Scafetta, P. Hamilton and P. Grigolini, *Fractals* **9**, 193 (2001); P. Grigolini, L. Palatella and G. Raffaelli, *Fractals* **9**, 439 (2001).
- [9] C.E. Shannon, *Bell Sys. Tech. J.* **27**, 379-423; *ibid* 623-656 (1948).
- [10] N. Wiener, *Time Series*, MIT Press, Cambridge (1949).
- [11] M. Ignaccolo, M. Latka and B.J. West, to be submitted to *Phys. Rev. Lett*, draft available at "arXiv.org" (arXiv:1001.4103).
- [12] In most practical application there is no difference between the overlapping and non-overlapping procedures aside from a better statistical result for the overlapping one.
- [13] M. Ignaccolo, P. Allegrini, P. Grigolini, P. Hamilton, and B. J. West, *Physica A*, **336**, 595 (2004); M. Ignaccolo, P. Allegrini, P. Grigolini, P. Hamilton, and B. J. West, *Physica A*, **336**, 623 (2004).
- [14] M. Ignaccolo, M. Latka, W. Jernajczyk, P. Grigolini and B. J. West, *J. of Biol. Phys.*, **36**, 185 (2010); M. Ignaccolo, M. Latka, W. Jernajczyk, P. Grigolini and B. J. West, *Physi. Rev. E*, in press.
- [15] M. Buiatti, P. Grigolini, and L. Palatella, *Physica A* **268**, 214 (1999).
- [16] G. Zumofen and J. Klafter, *Phys. Rev. E* **47**, 851 (1993).
- [17] P. Allegrini, J. Bellazzini, G. Bramanti, M. Ignaccolo, P. Grigolini, and J. Yan, *Phys. Rev. E* **66**, 015101, 2002.

- [18] R. C. Hwa and T. C. Ferree, *Phys. Rev. E* **66**, 021901 (2002).
- [19] M. Latka, M. Ignaccolo and B. J. West, under review *European Phys. Lett.*